NEOPLASIA
www.neoplasia.com

Volume 23 Number xxx Month 2021 pp. 993–1001

Original Research

Proprotein convertase subtilisin/kexin Type 9 is required for Ahnak-mediated metastasis of melanoma into lung epithelial cells ☆, ☆☆

Jung Min Suh [a,1]; Yelin Son [a,1]; Jung-Yeon Yoo [a]; Yookyung Goh [a]; Nabil G. Seidah [b]; Sanghyuk Lee [a,*]; Yun Soo Bae [a,*]

[a] Department of Life Science, Ewha Womans University, Seoul, Korea
[b] Laboratory of Biochemical Neuroendocrinology, Clinical Research Institute of Montreal, QC, Canada

Abstract

Previously we demonstrated that Ahnak mediates transforming growth factor-β (TGFβ)-induced epithelial-mesenchymal transition (EMT) during tumor metastasis. It is well-known that circulating tumor cells (CTCs) invade the vasculature of adjacent target tissues before working to adapt to the host environments. Currently, the molecular mechanism by which infiltrated tumor cells interact with host cells to survive within target tissue environments is far from clear. Here, we show that Ahnak regulates tumor metastasis through PCSK9 expression. To validate the molecular function of Ahnak in metastasis, B16F10 melanoma cells were injected into WT and Ahnak knockout (Ahnak$^{-/-}$) mice. Ahnak$^{-/-}$ mice were more resistant to the pulmonary metastasis of B16F10 cells compared to wild-type (WT) mice. To investigate the host function of Ahnak in recipient organs against metastasis of melanoma cells, transcriptomic analyses of primary pulmonary endothelial cells from WT or Ahnak$^{-/-}$ mice in the absence or presence of TGFβ stimulation were performed. We found PCSK9, along with several other candidate genes, was involved in the invasion of melanoma cells into lung tissues. PCSK9 expression in the pulmonary artery was higher in WT mice than Ahnak$^{-/-}$ mice. To evaluate the host function of PCSK9 in lung tissues during the metastasis of melanoma cells, we established lung epithelial cell-specific tamoxifen-induced PCSK9 conditional KO mice (Scgb1a1-Cre/PCSK9$^{fl/fl}$). The pulmonary metastasis of B16F10 cells in Scgb1a1-Cre/PCSK9$^{fl/fl}$ mice was significantly suppressed, indicating that PCSK9 plays an important role in the metastasis of melanoma cells. Taken together, our data demonstrate that Ahnak regulates metastatic colonization through the regulation of PCSK9 expression.

Neoplasia (2021) 23, 993–1001

Keywords: Ahnak, TGFβ, PCSK9, Extravasation, Metastasis

Introduction

Ahnak is a large protein (5890 amino acids, 629 kDa), the structure of which is divided into three domains: (1) the NH3-terminal domain (approximately 251 amino acids) contains the PSD-95/discs-large/ZO-1 (PDZ) domain; (2) the central region (251 amino acids) comprised of 36 repeating motifs that interact with phospholipase C-γ1 (PLCγ1), PKC, and Smad; and (3) the COOH-terminal region which consists of 1002 amino acids that provide a binding domain with the β2-subunit of the Ca_v channel, actin, and annexin [1-8]. These data implicate Ahnak as a molecular linker mediating various signaling networks. In previous work, Ahnak has been shown to occupy two different roles in cell signaling. Ahnak was identified as a PLCγ1 activator, mediating cell growth through IP3 and calcium signaling [2-4]. More recently, Ahnak was reported to suppress tumor growth through regulation of the TGFβ/Smad3 signaling cascade [5, 6]. These previous results suggest that Ahnak not only stimulates cell

* Corresponding author:
E-mail addresses: sanghyuk@ewha.ac.kr (S. Lee), baeys@ewha.ac.kr (Y.S. Bae).
☆ Funding: This work was supported by Aging project (2017M3A9D8062955 to YSB) and by Stem Cell grant (2017M3A9B3061850 to YSB) funded by Ministry of Science and ICT.
☆☆ Conflict of interest: The authors declare that they have no known competing financial interests or personal relationships that could have appeared to influence the work reported in this paper.
[1] These authors contributed equally to this work.
Received 24 March 2021; received in revised form 17 July 2021; accepted 19 July 2021

https://doi.org/10.1016/j.neo.2021.07.007

proliferation in response to growth factors including EGF and PDGF, but also suppresses cell growth by regulation of cytostatic factor such as TGFβ. TGFβ performs dual roles in cell proliferation [9-12]: (1) first as a cytostatic modulator during normal cell growth, and (2) second as a regulator for the metastasis of tumor cells. In the early stages of tumorigenesis, TGFβ has potent tumor suppressing activity. However, through the progression and advanced stages of cancer, TGFβ stimulates aggressive tumor development and induces metastasis including both intravasation and extravasation. Ahnak potentiates activity of TGFβ through interactions with R-Smads (Smad2 and Smad3) and I-Smad (Smad7). Therefore, the TGFβ-Ahnak signaling axis regulates EMT during tumor metastasis.

Extravasation of circulating tumor cells (CTCs) into target tissues is a critical event during metastasis for organ-specific homing [13-18]. CTCs bind to adhesion molecules on endothelial cells and transmigrate into the sub-endothelium. Various reports have suggested that TGFβ not only mediates the epithelial-mesenchymal transition (EMT) of CTCs, but also regulates the metastatic signature of host cells. Infiltrated tumor cells need to adapt to and interact with the new stromal environments. Tumor cells secrete developmental and self-renewal signals such as hedgehog, Wnt, TGFβ, and chemokines in order to create favorable microenvironments. In this report, we first show that the Ahnak-TGFβ axis regulates the metastatic signature of lung epithelial cells including PCSK9 expression. We present the role of PCSK9 in lung metastasis of melanoma cells with lung epithelial cells-specific PCSK9 conditional KO mice. These results provide novel insights into the Ahnak-TGFβ axis and its role in the regulation of infiltrated tumor cell colonization.

Materials and methods

Materials

Recombinant human TGFβ1 (Catalog number: 240-B) was purchased from R&D Systems. An antibody against Ahnak was generated by using a synthetic KIS peptide according to a previous report by Young In Frontier (Rep. of Korea). The following antibodies were also used: PCSK9 (MA5-32843, Invitrogen), Scgb1a1 (PAS-102469, Invitrogen). Tetramethyl rhodamine isothiocyanate (TRITC)-labelled mouse and rabbit secondary antibodies were purchased from Kirkegaard & Perry Laboratories (KPL). FITC Annexin V Apoptosis Detection kit I (556547, BD Bioscience) and 7-AAD (559925, BD Bioscience) were purchased from BD Bioscience.

Mice

All animal procedures were approved by the Institutional Animal Care and Use Committee (IACUC) at Ewha Womans University. Mice were housed in specific pathogen-free environment under a 12 hrs light and/or dark cycle. Animal protocols including food and water were in compliance with NIH Guideline for the Care and Use of Laboratory Animals and have been approved by the IACUC of Center for Laboratory Animal Sciences, Ewha Industry-University Cooperation Foundation, Ewha Womans University.

Generation of lung epithelium PCSK9 conditional knockout mice

Lung epithelial cell-specific Scgb1a1 promoter-driven inducible Cre recombinase-estrogen receptor fusion protein (CreER) transgenic mouse (Scgb1a1-CreER) was crossed with *Pcsk9*$^{fl/fl}$ mice [19]. For PCSK9 depletion, Scgb1a1^{CreER}/ PCSK9$^{fl/fl}$ mice were intraperitoneal injected with tamoxifen (75 mg/kg) once a day for 5 times. The final tamoxifen administration was 1 wk before the melanoma injection.

Lung metastasis study

Melanoma B16F10 cells were prepared in 5×10^5 cells per mouse injections suspended in 100 μL of PBS. For tail vein injections, 6- to 8-wk-old male mice were restrained using a rodent restrainer. The mouse tail was kept in contact with a 40 °C heat pad to relax the vein before injection. Cells were injected into the mouse using a 30.5-gauge needle. Fourteen days later, mice were sacrificed and perfused with PBS through the right ventricle until pulmonary blood was completely removed. Lung tissues were preserved in 10% neutral buffered formalin (NBF), and tumor colonies on the lung surface were counted. GraphPad Prism software was used for statistical assessments and graphical presentations of colony number. Median values and statistical significance were obtained with Student's *t* test and the Mann-Whitney U test. Scgb1a1-creER and Scgb1a1-creER/PCSK9$^{fl/fl}$ mice were injected intravenously with 2×10^6 control B16F10 cells per mouse. After fifteen days, mice were sacrificed and the lung tissues were analyzed by the method described above.

Isolation of mouse pulmonary endothelial cell

Mouse pulmonary endothelial cells were isolated from the lungs of 6- to 8-wk-old WT or Ahnak$^{-/-}$ mice. Each mouse was sacrificed by CO_2 inhalation. After reperfusion with PBS, the lungs were removed and digested in DMEM supplemented with 0.1% type I collagenase (Worthington) for 60 minutes at 37 °C. A total of 15 mL of collagenase solution was used per mouse, and the mixture was shaken vigorously during digestion before being titrated into the fixed cannula 3 times. The collagenase solution containing cells was then strained through a 70-μm strainer. The filtered cell suspension was centrifuged at 1300 rpm for 8 minutes. After removal of the supernatant, the cell pellet was resuspended twice in 20 mL of 10% DMEM and again centrifuged at 1300 rpm for 8 minutes. After the supernatant was removed, the cell pellet was resuspended in 4 mL of 10% DMEM, and Dynabeads (Invitrogen) coupled to an anti-ICAM-2 antibody were added to the cells. The Dynabeads and/or cell mixture was incubated for 30 minutes at 4 °C. The bead-bound cells were collected using a magnet, washed 5 times in 10% DMEM and once in serum-free DMEM, and digested for 8 minutes at 37 °C in 1 mL of trypsin/EDTA to release the beads from the cells. The bead-free cells in 10% DMEM were centrifuged, resuspended in 4 mL of EGM-2 culture medium (Lonza), plated onto a gelatin-coated 60 mm culture dish, and left undisturbed for approximately 4 to 5 days.

Transcriptome sequencing and data analysis

The cDNA libraries were constructed with the TruSeq mRNA library kit using 1 μg of total RNA. Paired end sequencing of 100-mers length was performed using an Illumina HiSeq4000 system. On average, we generated 44.6 million reads for each sample. Transcript abundance was estimated using the MapSplice-RSEM pipeline [20, 21]. RNA-seq reads were mapped to the mouse genome (GRCm38/mm10) using MapSplice2, and reads with indels, large inserts, and zero mapping quality were filtered out with Ubu-1.2. We then used RSEM to calculate the mRNA expression at the gene level. Expected counts from the RSEM output were normalized using the upper quartile method after filtering low count reads and taking the logarithm. Differentially expressed genes (DEGs) were obtained by fitting logarithmic curves to the MA plot for comparing gene expression before and after TGFβ treatment in WT and Ahnak$^{-/-}$ mice (Supplementary Fig. 1). The RNA-Seq data have been deposited in the Gene Expression Omnibus (GEO) database [GEO: GSE167195].

Histological analysis

Lung tissues from WT or Ahnak$^{-/-}$ mice were fixed with 10% NBF solution overnight at room temperature. After serial processing of samples by dehydration in a graded alcohol series and subsequent clearing, tissues were embedded in paraffin. Tissue sections were cut at a thickness of 4 μm. Antigens in the lung sections were retrieved in a sodium citrate buffer by boiling for 20 minutes. Endogenous peroxidase activity was blocked by incubation with 0.3% H_2O_2 for 10 minutes. Nonspecific antibody binding was blocked with Protein Block Serum-Free Ready-to-use (Dako) for 30 minute at room temperature. The PCSK9 primary antibody was bound to tissues for 16 h at 4 °C. The HRP-conjugated secondary antibodies were incubated with tissues for 1 h at room temperature. Liquid DAB+ Substrate Chromogen System (Dako) was utilized for horseradish peroxidase (HRP)-based immunodetection. Images were recorded using a light microscope (ECLIPSE 81i, Nikon). To quantify PCSK9 expression in mouse lung tissues, Image-Pro Analyzer 7.0 was utilized. Briefly, PCSK9-stained areas in each pulmonary artery were identified and divided by the area of the lung (5 areas from WT and three areas from Ahnak$^{-/-}$ mice). Then, the mean ± S.D. was calculated, and statistical significance was analyzed with Student's *t* test.

Cell culture and Western blot

The BEAS-2B cells were purchased from ATCC and cultured at 37°C in BEGM Bronchial epithelial cell growth medium bullet kit (CC-3170, Lonza) following manufacturer's instruments. The cells were incubated with or without SB431542 (S4317, Sigma Aldrich) in response to TGFβ1 (240-B, R&D systems). The concentrated supernatant and cell lysates of BEAS-2B were subjected to SDS-PAGE and transferred to nitrocellulose membrane. Immunoblot was performed with antibody against PCSK9 and the bands were visualized by chemiluminescence (Amersham Imager 600).

Apoptosis assay by flow cytometry

B16F10 melanoma cells were seeded at 5 × 10^5 per well in 12 well plate. When the cell density reached to 70%, the cells were treated with 5 μg cycloheximide and 30 ng/ml TNFα in the absence or presence of 2 ng/ml recombinant PCSK9 for 24 hrs. The cells were trypsinized, washed with cold PBS and incubated with binding buffer containing Annevin V and 7-AAD. Flow cytometry analysis was performed by FACS Calibur (BD Bioscience, San Jose, CA, USA).

Statistics

Statistical analysis was performed with a two-tailed unpaired *t* test. Data are presented as the mean ± SD of values obtained from 3 to 5 independent experiments. All western blots in figures are representative of three independent experiments.

Results

Suppression of lung metastasis and transcriptomic analyses in Ahnak$^{-/-}$ mice

To validate the host function of Ahnak during extravasation of CTCs into lung tissues, we injected B16F10 melanoma cells into WT or Ahnak knockout (Ahnak$^{-/-}$) mice and analyzed lung metastasis. B16F10-injected WT mice developed multiple lung metastatic nodules, whereas Ahnak$^{-/-}$ mice were resistant to lung metastasis (Fig. 1). To investigate the molecular mechanisms underlying the extravasation process, we produced RNA sequencing data from primary pulmonary endothelial cells (ECs) harvested from WT and Ahnak$^{-/-}$ mice in the absence or presence of TGFβ stimulation. From transcriptome analyses, we obtained 1984 differentially expressed genes (DEGs) on TGFβ stimulation in WT ECs (Supplementary Fig. S1A). We then filtered out genes that were also DEGs in ECs of Ahnak$^{-/-}$ mice on TGFβ stimulation (Supplementary Fig. S1B). The remaining DEGs were regarded as the Ahnak-dependent DEG set, the primary target of this study. We obtained 387 upregulated and 648 downregulated Ahnak-dependent DEGs on TGFβ stimulation (Supplementary Table S1).

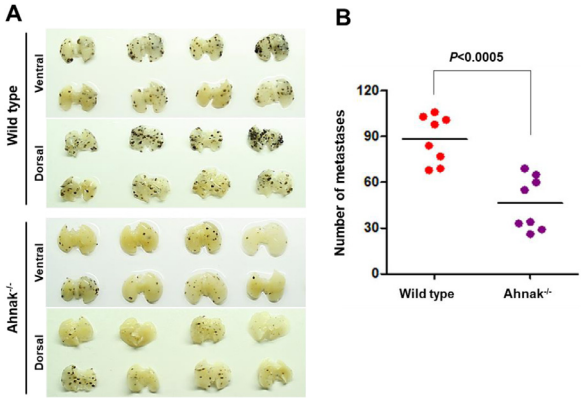

Fig. 1. Host Ahnak function in pulmonary endothelial cells during extravasation of B16F10 melanoma cells. (A) B16F10 melanoma cells were inoculated into 8 to 10-wk-old male WT and Ahnak$^{-/-}$ mice via tail vein injection. The mice were sacrificed after fourteen days. The representative photograph is of the dorsal side of a lung with metastatic lesions. (B) The number of metastatic colonies was counted and statistically analyzed using the Mann-Whitney U test.

To gain insight into the biological functions of Ahnak-dependent DEGs, we performed gene set over-representation analysis using the DAVID Bioinformatics Resource (Ver. 6.8) [22]. Top scoring functional clusters for upregulated genes were related to VEGF signaling and angiogenesis (Fig. 2A). Down-regulated genes were enriched in cilium-related processes (Supplementary Fig. S2). Representative enriched processes included angiogenesis via VEGF signaling (functional cluster 1 & 2), DNA base synthesis (functional cluster 3), and DNA damage response (functional cluster 4) that would play essential roles in growth of metastatic tumor. Thus, our transcriptome data highlight molecular features in the extravasation step of metastasis. Identifying key regulators among several hundred DEGs is an important yet challenging task, given the limited amount of data. The difference score in $\log_2$FoldChange between WT and Ahnak$^{-/-}$ mice, called as 'the fold difference', represents the contribution of each gene to the phenotype in an Ahnak-dependent manner (Fig. 2B). Thus, we sorted the Ahnak-dependent DEGs according to the fold difference and annotated gene functions manually (Fig. 2B). Many high-scoring genes belonged to the biological processes identified from the gene set analysis, thus supporting the fold difference as a surrogate measure of critical features in metastasis.

PCSK9 is involved in lung metastasis in Ahnak$^{-/-}$ mice

Among the enriched functional clusters from the DAVID analysis, functional cluster 5 on 'cholesterol and steroid metabolism' was an unexpected feature to be involved in the metastatic process (Fig. 2A). We focused on Proprotein Convertase Subtilisin/Kexin Type 9 (PCSK9), primarily known to regulate cholesterol homeostasis, because PCSK9 was one of the top candidates in the fold difference score (Fig. 2B). Furthermore, previous reports showed that PCSK9 deficiency reduced melanoma metastasis in the liver and that PCSK9-/- mice were more resistant to liver metastasis of

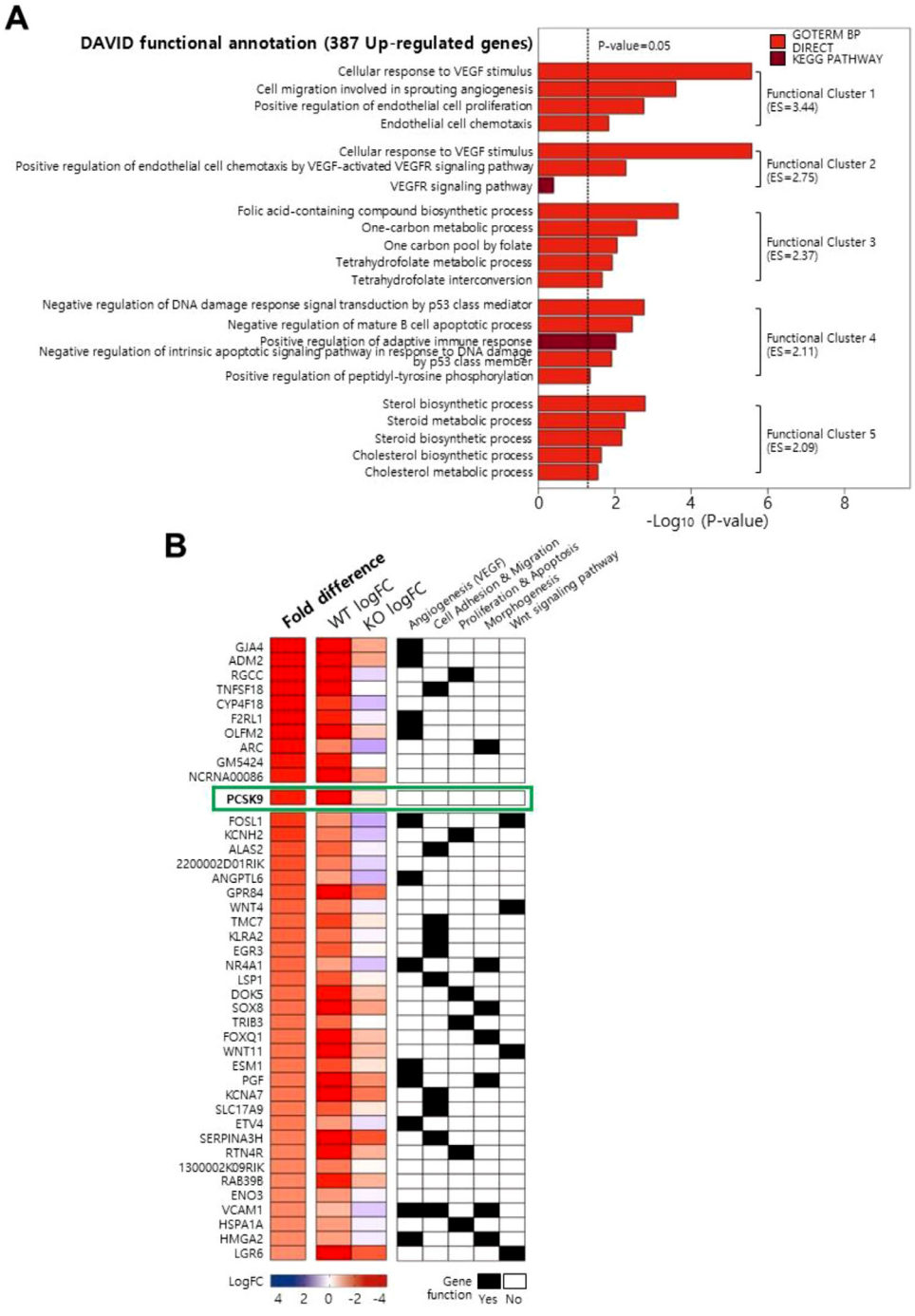

Fig. 2. Transcriptome analysis of pulmonary endothelial cells from WT and Ahnak KO mice. (A) Functional enrichment analysis result from DAVID web service (ver. 6.8) for upregulated genes. Biological processes in the Gene Ontology and KEGG pathways were used as input gene sets and 5 top-scoring functional clusters were included in the bar plot. (B) Top 42 genes sorted in the fold difference score. Fold difference and log fold changes in wild-type and KO mice are shown in the heatmap. Functional annotation was done manually.

B16F1 cells [23, 24]. Thus, we hypothesized that PCSK9 might play key roles in pulmonary metastases of melanoma cells in an Ahnak-dependent way.

We then performed a series of experiments to validate roles of PCSK9 in metastasis. First, we measured PCSK9 expression in pulmonary endothelial cells by staining the pulmonary artery with an antibody specific to PCSK9. PCSK9 expression in the pulmonary artery was higher in WT mice than in Ahnak$^{-/-}$ mice (Figs. 3A, B). Moreover, immunoblot results of lung tissues marked with an antibody against PCSK9 clearly demonstrated that PCSK9 expression was suppressed in Ahnak$^{-/-}$ mice (Fig. 3C). Moreover, PCSK9 expression was increased in response to TGFβ in BEAS-2B bronchial epithelial cells and its expression was suppressed by the pre-treatment of SB431542, specific TGFβR1 inhibitor, indicating that the expression of PCSK9 was regulated by TGFβ and its downstream signaling cascade (Fig. 3D).

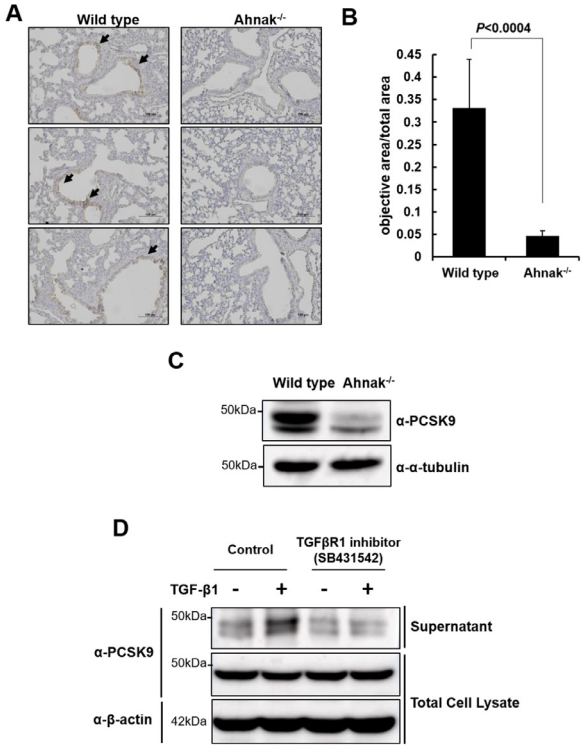

Fig. 3. PCSK9 expression in WT and Ahnak$^{-/-}$ mice. (A) PCSK9 expression in the pulmonary arteries from WT and Ahnak$^{-/-}$ mice. Arrow means PCSK9 expression in IHC. (B) Quantitation of PCSK9 expression in (A). (C) Lysates of lung bronchial tissues from WT and Ahnak$^{-/-}$ mice were subjected into immunoblot analysis with antibody to Ahnak. (D) Immunoblot for PCSK9 secretion in response to TGFβ in the absence or presence of TGFβR1 inhibitor.

Validation of PCSK9 function in lung metastasis of melanomas

Next, we evaluated PCSK9 function during the lung metastasis of B16F10 cells using lung epithelial cell-specific conditional KO (cKO) mice. We established a tamoxifen-induced lung epithelial cell-specific PCSK9 conditional KO mice (Scgb1a1-CreER/PCSK9$^{fl/fl}$) [19] (Fig. 4A). Scgb1a1 (secretoglobin) is expressed in non-ciliated Clara cells and Cre recombinase activity of Scgb1a1-CreER strain is specifically increased in lung epithelial cells upon tamoxifen injection [25], leading to the deletion of PCSK9 gene. We found that protein level of PCSK9 in tissue lysates of lung and liver from WT or tamoxifen-untreated Scgb1a1-CreER/PCSK9$^{fl/fl}$ mice was not significantly different. On the other hand, the level of PCSK9 protein in lung tissues from tamoxifen-injected Scgb1a1-CreER/PCSK9$^{fl/fl}$ mice was significantly lower than that of WT mice (Fig. 4B). Remained PCSK9 in lung lysates from tamoxifen-injected Scgb1a1-CreER/PCSK9$^{fl/fl}$ mice was likely originated from pulmonary endothelial cells, fibroblasts, and alveolar macrophages. To validate lung epithelial cell-specific knockout of PCSK9 protein, we performed immunohistochemistry (IHC) with antibody to PCSK9 in Scgb1a1-CreER/PCSK9$^{fl/fl}$ mice with or without tamoxifen injection. The tamoxifen-untreated lung epithelial cells in Scgb1a1-CreER/PCSK9$^{fl/fl}$ mice clearly expressed PCSK9 protein. However, PCSK9 expression was abolished in tamoxifen-injected Scgb1a1-CreER/PCSK9$^{fl/fl}$ mice (Fig. 4C). Next, we investigated the function of PCSK9 in lung metastasis of B16F10 melanoma cells. Injection of B16F10 cells into tamoxifen-treated Scgb1a1-CreER/PCSK9$^{fl/fl}$ mice resulted in suppressed lung metastasis compared to both WT and tamoxifen-untreated Scgb1a1-CreER/PCSK9$^{fl/fl}$ mice (Figs. 4D, E).

To investigate the molecular mechanism in which PCSK9 is involved in lung metastasis of B16F10 cells, we performed tumor necrosis factor-α (TNFα)-mediated apoptosis of melanoma cells in the presence of PCSK9. Addition of recombinant PCSK9 into melanoma cells resulted in reduced TNFα-mediated apoptosis of melanoma cells (Fig. 5A). Moreover, TNFα stimulated the generation of active Caspase 3, whereas PCSK9 suppressed it (Fig. 5B), indicating that PCSK9 serves as inhibitor for TNFα-mediated apoptosis during lung metastasis of B16F10 cells. However, the detailed molecular mechanisms by which the PCSK9 regulates TNFα-mediated apoptosis remains to be elucidated.

Discussion

Metastasis is regulated by a complex series of biochemical and cellular level events [13-16]. Tumor cells leaving the primary site is first vital step in metastasis. Although various cytokines, growth factors, and adhesion molecules have been reported to be involved in the metastasis process, the role of TGFβ has been exceedingly well established. TGFβ serves not only as a cytostatic cytokine during normal growth, but also as a tumor growth factor in metastasis [9-12]. During metastasis, TGFβ regulates EMT, allowing tumor cells to leave the primary site and invade towards the blood vessels. The second important event is intravasation; single tumor cells express and secrete angiogenesis factors and metalloproteinase in order to disrupt the endothelial junctions of blood vessels, providing a migration path for tumor cells to enter the bloodstream. Because infiltrated tumor cells face a harsh environment in bloodstream where they are subject to heavy immune surveillance, most cells are eliminated by the immune system. However, the remaining tumor cells aggressively invade secondary organ site in a process called extravasation, adhesion to the target organ is a first critical step. Host endothelial cells express a variety of adhesion proteins such as E-selectin, P-selectin, VCAM-1 and ICAM-1. Binding of these adhesion molecules with ligands on the surface of tumor cells allow the cells to overcome the mechanical pressure in the bloodstream and invade towards the target organ. After extravasation, secretion of exosome-containing pro-inflammatory cytokines such as macrophage inhibitory factor (MIF) provides pre-metastatic niches for tumor cell growth. These microenvironments support the expression of the Wnt, TGFβ, STAT3, PI3K and HIF pathways which facilitate the colonization of infiltrated tumor cells.

As discussed earlier in this article, TGFβ is known to be an important cytokine during whole the process of metastasis [9-12]. Our 2 previous reports indicated that Ahnak binds and stimulates TGFβ-mediated signaling cascades including activation of Smad2/3 and expression of c-Myc [5, 6]. In line with the "seed-and-soil" hypothesis of tumor metastasis, our previous reports investigated the "seed" function of Ahnak in tumor cells. As we shown before, Ahnak regulated EMT in HaCaT keratinocytes and B16F10 melanoma cells in response to TGFβ [6]. EMT characteristics such as cell invasion activity and expression of various EMT marker genes are suppressed in Ahnak knockdown HaCaT keratinocytes and B16F10 cells [6]. Injection of B16F10-shAhnak cells resulted in significantly reduced lung metastasis, suggesting that the TGFβ-Ahnak signaling axis regulates EMT during tumor metastasis. In this report, we examined the "soil" function of Ahnak in lung endothelial cells in the absence or presence of TGFβ. To that end, Ahnak-TGFβ axis-dependent DEGs were identified and shown to be associated with the VEGF pathway (Fig. 2). Intravasation requires expression of angiogenic factors such as VEGF, FLT1, and KDR. Expression of VEGF and its receptors is attenuated in Ahnak-deficient ECs in response to TGFβ, indicating that the Ahnak-TGFβ axis contributes to supporting a favorable environment for intravasation. Cell-cell adhesion and migration-associated DEGs were also identified (Fig. 2B). The expression of adhesion molecules in the target organ provides the binding sites required for CTCs. Interaction of adhesion molecules with the ligands of CTCs is the first step of extravasation, resulting in tumor cells attached the surface of target organ. This interaction allows

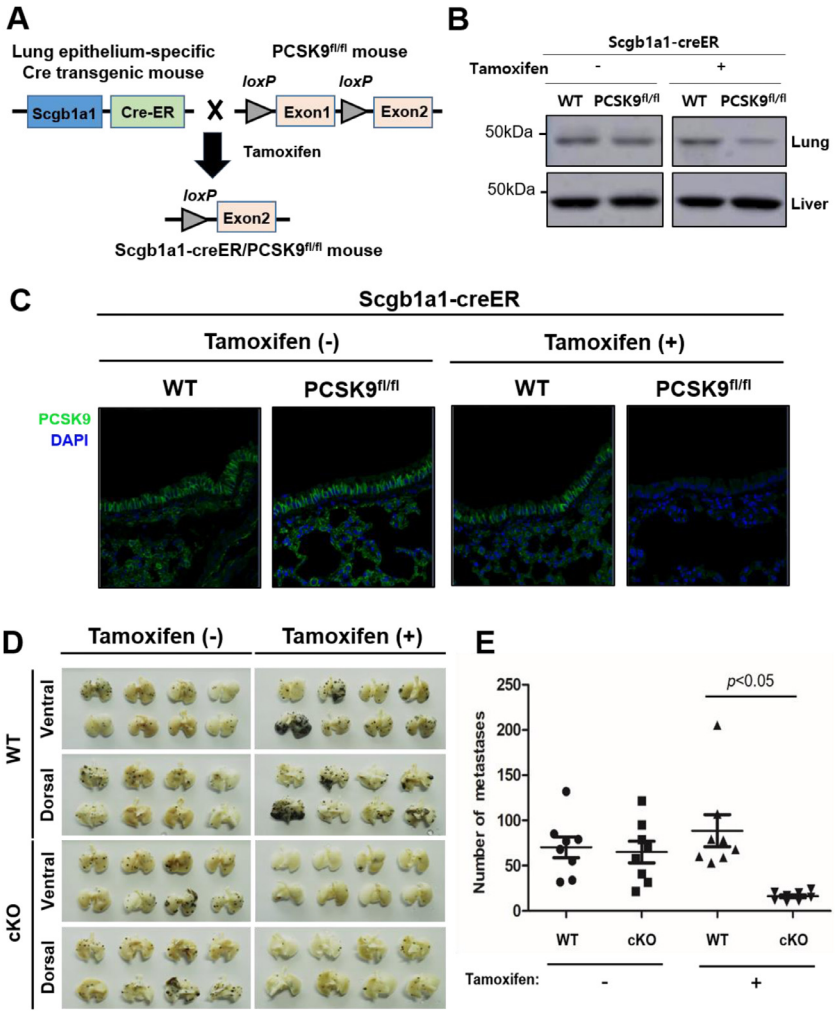

Fig. 4. Generation and evaluation of tumor metastasis in Scgb1a1-Cre/PCSK9$^{fl/fl}$ mice. (A) Strategy of generating lung epithelium-specific PCSK9 conditional KO mice. Lung epithelial cell-specific Scgb1a1 promoter-driven inducible Cre recombinase-estrogen receptor fusion protein (CreER) transgenic mouse (Scgb1a1-CreER) was crossed with *Pcsk9$^{fl/fl}$* mice [19]. For PCSK9 depletion, Scgb1a1^{CreER}/ PCSK9$^{fl/fl}$ mice were intraperitoneal injected with tamoxifen (75 mg/kg) once a day for five times. (B) Lysates of lung bronchial tissues from Scgb1a1-Cre mice (control) and Scgb1a1-Cre/PCSK9$^{fl/fl}$ mice were subjected into immunoblot analysis with an antibody to PCSK9. (C) Immunochemistry with antibody to PCSK9 in lung bronchial tissues from Scgb1a1-Cre and Scgb1a1-Cre/PCSK9$^{fl/fl}$ mice. (D) B16F10 melanoma cells were inoculated into 8-wk-old male Scgb1a1-Cre and Scgb1a1-Cre/PCSK9$^{fl/fl}$ mice via tail vein injection. The mice were sacrificed after fourteen days. The representative photograph is the dorsal side of a lung with metastatic lesions. (E) The number of metastatic colonies was counted and statistically analyzed with the Mann-Whitney U test.

the tumor cells to overcome mechanical forces in the bloodstream and to migrate through endothelium. These results indicate that Ahnak regulates intravasation and extravasation in the metastasis of tumor cells (Fig. 5C).

Proprotein convertase subtilisin/kexin type 9 (PCSK9) is a secretory serine protease strongly associated with the regulation of low-density lipoprotein receptor (LDLR) levels [26]. PCSK9 binds to the LDLR on the cell surface and mediates LDLR degradation through clathrin-mediated internalization and endosomal compartmentation [27]. A gain-of-function mutation in PCSK9 is associated with familial hypercholesterolemia and a loss-of-function mutation is involved in reduced LDL cholesterol levels [27]. PCSK9 was originally identified as neural apoptosis-regulated candidate-1 [26] and was also reported to be involved in anti-apoptotic signaling [24, 28]. While the gain-of-function PCSK9 mutation (D349Y) was shown to reduce the expression of pro-apoptotic genes, apoptosis was reported to be enhanced during liver regeneration in PCSK9-deficient mice [19, 29]. High PCSK9 expression in the liver is associated with the metastatic activity of B16F10 melanoma cells [24]. PCSK9 itself did not affect the apoptosis of B16F10 melanoma cells, but demonstrated a regulatory function in the development of metastasis through the apoptosis of host cells [24]. PCSK9 deficiency in host cells resulted in a strong response to TNFα stimulation, leading to cell death [24]. Our results indicate that the down-regulation of PCSK9 expression in pulmonary endothelial cells of Ahnak$^{-/-}$ mice resulted in decreased lung metastasis of B16F10 melanoma cells (Fig. 3). As our results show, the function of host PCSK9 during metastasis in lung tissue is similar to that during liver metastasis. While our results show strong evidence of PCSK9 involvement during tumor metastasis, the detailed molecular mechanisms by which the PCSK9 deficiency in Ahnak$^{-/-}$ mice attenuated the metastasis of melanoma cells remains to be elucidated.

Cholesterol and its metabolites serve as components of biological membrane and as presursors of hormones regulating biological functions and cell proliferation. On the other hand, cholesterol metabolism can also regulate signaling networks to mediate tumorigenesis and tumor environments. Our previous reports indicated that Ahnak$^{-/-}$ mice were resistant to high fat diet (HFD)-induced obesity and fat accumulation [30, 31]. The lipid metabolism

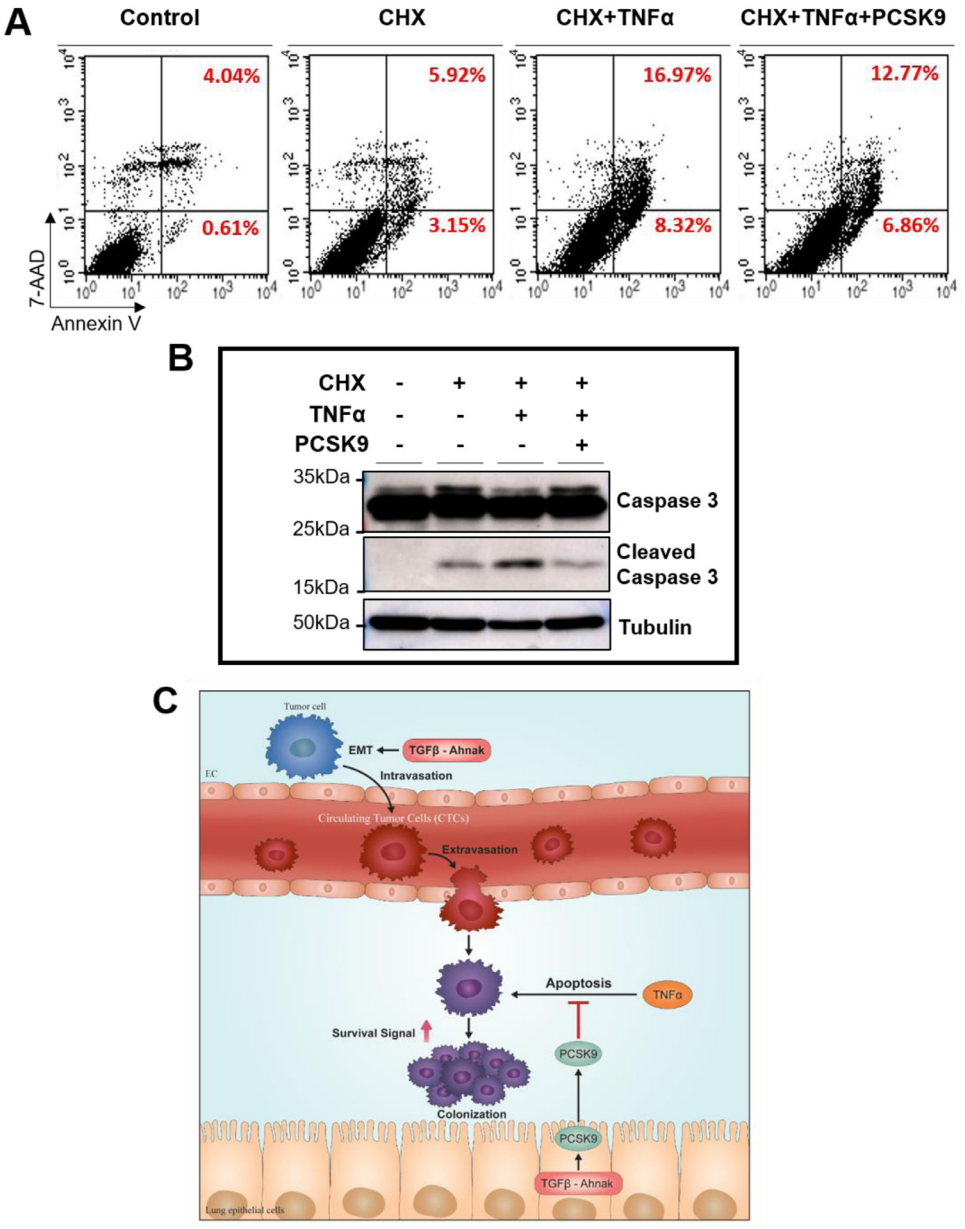

Fig. 5. PCSK9 regulates TNFα-mediated apoptosis and putative model of Ahnak/PCSK9-dependent metastasis. (A) FACS analysis for TNFα-mediated apoptosis. B16F10 melanoma cells were treated with 5 μg cycloheximide and 30 ng/ml TNFα in the absence or presence of 2 ng/ml recombinant PCSK9 for 24 hrs. The cells were incubated with binding buffer containing Annevin V and 7-AAD. Flow cytometry analysis was performed by FACS Calibur (BD Bioscience, San Jose, CA, USA). (B) PCSK9 suppressed TNFα-dependent active Caspase 3 generation. B16F10 melanoma cells were treated with 5 μg cycloheximide and 30 ng/ml TNFα in the absence or presence of 2 ng/ml recombinant PCSK9 for 24 hrs. The lysates of B16F10 melanoma cells were subjected into immunoblot with antibody against Caspase 3. (C) Putative model of Ahnak-dependent metastasis. Ahnak is associated with tumor metastasis through the induction of PCSK9. Downregulated expression of PCSK9 in pulmonary endothelial cells of Ahnak$^{-/-}$ mice attenuates the lung metastasis activity of B16F10 melanoma cells. These results indicate that Ahnak plays an important role in extravasation of CTCs into pulmonary endothelial cells through the regulation of PCSK9 expression.

parameters including triglyceride, cholesterol, and LDL-cholesterol were substantially decreased in HFD-fed Ahnak$^{-/-}$ mice, compared to that in WT [30]. Moreover, we found that Ahnak-mediated BMP-Smad signaling networks regulated adipogenesis and adipocyte differentiation [30, 32]. In according to metabolomics data from 600-MHz ^{1}H NMR spectra for urine from WT and Ahnak$^{-/-}$ mice on HFD, threonine and histidine related to fatty acid metabolism were elevated in the urine of HFD-fed Ahnak$^{-/-}$ mice [31]. Based on these results, we found that the TGFβ-mediated cholesterol and lipid metabolism in Ahnak$^{-/-}$ mice were suppressed. Moreover, the level of PCSK9 was downregulated in Ahnak$^{-/-}$ mice, suggesting that the level of cholesterol was suppressed in Ahnak-deficient mice (Fig. 2 and 3). It was established that PCSK9 can stimulate the degradation of LDLR which is essential for tumorigenesis [33, 34]. The roles of PCSK9 in cancer have been highlighted recently in terms of regulation of inflammation via SOCS3-STAT3 pathway [35] and cell proliferation and apoptosis [36]. Moreover, the deficiency of PCSK9 was shown to prevent tumor growth in a

manner that depends on cytotoxic T cells that further implicated applications in cancer immunotherapy [37]. Taken together, the reduction of PCSK9 level in Ahnak$^{-/-}$ mice is considered to inhibit tumor progression and metastasis.

In this study, we report the signaling mechanisms that illustrate the significance of Ahnak in malignant tumors (Fig. 5C). TGFβ-Ahnak axis stimulated PCSK9 expression and secreted PCSK9 suppressed TNFα-mediated apoptosis of melanoma cells, providing a possible molecular mechanism by which Ahnak-PCSK9 regulates lung metastasis of melanoma cells. We also clearly demonstrate that Ahnak promotes TGFβ-induced EMT and cancer metastasis, suggesting that Ahnak may be a useful prognostic marker in cancer treatment. To further investigate the value of Ahnak as a prognostic marker in malignant tumor, analysis of dysregulated Ahnak expression is required to better illustrate the biochemical mechanisms underlying Ahnak activity. Finally, we propose that Ahnak may be an important therapeutic target for cancer treatment.

Supplementary materials

Supplementary material associated with this article can be found, in the online version, at doi:10.1016/j.neo.2021.07.007.

References

[1] Davis TA, Loos B, Engelbrecht AM. AHNAK: The giant jack of all trades. *Cell Signal* 2014;**26**:2683–93.

[2] Sekiya F, Bae YS, Jhon DY, Hwang SC, Rhee SG. AHNAK, a protein that binds and activates phospholipase C-gamma1 in the presence of arachidonic acid. *J Biol Chem* 1999;**274**:13900–7.

[3] Lee IH, You JO, Ha KS, Bae DS, Suh PG, Rhee SG, Bae YS. AHNAK-mediated activation of phospholipase C-gamma1 through protein kinase C. *J Biol Chem* 2004;**279**:26645–53.

[4] Lee IH, Lim HJ, Yoon S, Seong JK, Bae DS, Rhee SG, Bae YS. Ahnak protein activates protein kinase C (PKC) through dissociation of the PKC-protein phosphatase 2A complex. *J Biol Chem* 2008;**283**:6312–20.

[5] Lee IH, Sohn M, Lim HJ, Yoon S, Oh H, Shin S, Shin JH, Oh SH, Kim J, Lee DK, et al. Ahnak functions as a tumor suppressor via modulation of TGFbeta/Smad signaling pathway. *Oncogene* 2014;**33**:4675–84.

[6] Sohn M, Shin S, Yoo JY, Goh Y, Lee IH, Bae YS. Ahnak promotes tumor metastasis through transforming growth factor-beta-mediated epithelial-mesenchymal transition. *Sci Rep* 2018;**8**:14379.

[7] Matza D, Flavell RA. Roles of Ca(v) channels and AHNAK1 in T cells: the beauty and the beast. *Immunol Rev* 2009;**231**:257–64.

[8] Hu W, Bhattacharya S, Hong T, Wong P, Li L, Vaidehi N, Kalkum M, Shively JE. Structural characterization of a dimeric complex between the short cytoplasmic domain of CEACAM1 and the pseudo tetramer of S100A10-Annexin A2 using NMR and molecular dynamics. *Biochim Biophys Acta Biomembr* 2021;**1863**:183451.

[9] Batlle E, Massague J. Transforming growth factor-beta signaling in immunity and cancer. *Immunity* 2019;**50**:924–40.

[10] Zi Z, Chapnick DA, Liu X. Dynamics of TGF-beta/Smad signaling. *FEBS Lett* 2012;**586**:1921–8.

[11] Drabsch Y, ten Dijke P. TGF-beta signalling and its role in cancer progression and metastasis. *Cancer Metastasis Rev* 2012;**31**:553–68.

[12] Moustakas A, Heldin CH. Mechanisms of TGFbeta-induced epithelial-mesenchymal transition. *J Clin Med* 2016;**5**:63.

[13] Fares J, Fares MY, Khachfe HH, Salhab HA, Fares Y. Molecular principles of metastasis: A hallmark of cancer revisited. *Signal Transduct Target Ther* 2020;**5**:28.

[14] Gao Y, Bado I, Wang H, Zhang W, Rosen JM, Zhang XH. Metastasis organotropism: Redefining the congenial soil. *Dev Cell* 2019;**49**:375–91.

[15] Strilic B, Offermanns S. Intravascular survival and extravasation of tumor cells. *Cancer Cell* 2017;**32**:282–93.

[16] Massague J, Obenauf AC. Metastatic colonization by circulating tumor cells. *Nature* 2016;**529**:298–306.

[17] Reymond N, d'Agua BB, Ridley AJ. Crossing the endothelial barrier during metastasis. *Nat Rev Cancer* 2013;**13**:858–70.

[18] Labelle M, Hynes RO. The initial hours of metastasis: the importance of cooperative host-tumor cell interactions during hematogenous dissemination. *Cancer Discov* 2012;**2**:1091–9.

[19] Zaid A, Roubtsova A, Essalmani R, Marcinkiewicz J, Chamberland A, Hamelin J, Tremblay M, Jacques H, Jin W, Davignon J, et al. Proprotein convertase subtilisin/kexin type 9 (PCSK9): hepatocyte-specific low-density lipoprotein receptor degradation and critical role in mouse liver regeneration. *Hepatology* 2008;**48**:646–54.

[20] Wang K, Singh D, Zeng Z, Coleman SJ, Huang Y, Savich GL, He X, Mieczkowski P, Grimm SA, Perou CM, et al. MapSplice: accurate mapping of RNA-seq reads for splice junction discovery. *Nucleic Acids Res* 2010;**38**:e178.

[21] Li B, Dewey CN. RSEM: Accurate transcript quantification from RNA-Seq data with or without a reference genome. *BMC Bioinformatics* 2011;**12**:323.

[22] Huang DW, Sherman BT, Tan Q, Kir J, Liu D, Bryant D, Guo Y, Stephens R, Baseler MW, Lane HC, et al. DAVID bioinformatics resources: Expanded annotation database and novel algorithms to better extract biology from large gene lists. *Nucleic Acids Res* 2007;**35**:W169–75.

[23] Gangloff A, Calon F, Seidah NG. Can iPCSK9-induced hypocholesterolemia starve cancer cells? *J Clin Lipidol* 2017;**11**:600–1.

[24] Sun X, Essalmani R, Day R, Khatib AM, Seidah NG, Prat A. Proprotein convertase subtilisin/kexin type 9 deficiency reduces melanoma metastasis in liver. *Neoplasia* 2012;**14**:1122–31.

[25] Rawlins EL, Okubo T, Xue Y, Brass DM, Auten RL, Hasegawa H, Wang F, Hogan BL. The role of Scgb1a1+ Clara cells in the long-term maintenance and repair of lung airway, but not alveolar, epithelium. *Cell Stem Cell* 2009;**4**:525–534.

[26] Seidah NG, Benjannet S, Wickham L, Marcinkiewicz J, Jasmin SB, Stifani S, Basak A, Prat A, Chretien M. The secretory proprotein convertase neural apoptosis-regulated convertase 1 (NARC-1): Liver regeneration and neuronal differentiation. *Proc Natl Acad Sci U S A* 2003;**100**:928–33.

[27] Seidah NG, Abifadel M, Prost S, Boileau C, Prat A. The proprotein convertases in hypercholesterolemia and cardiovascular diseases: Emphasis on proprotein convertase Subtilisin/Kexin 9. *Pharmacol Rev* 2017;**69**:33–52.

[28] Wu CY, Tang ZH, Jiang L, Li XF, Jiang ZS, Liu LS. PCSK9 siRNA inhibits HUVEC apoptosis induced by ox-LDL via Bcl/Bax-caspase9-caspase3 pathway. *Mol Cell Biochem* 2012;**359**:347–58.

[29] Canuel M, Sun X, Asselin MC, Paramithiotis E, Prat A, Seidah NG. Proprotein convertase subtilisin/kexin type 9 (PCSK9) can mediate degradation of the low density lipoprotein receptor-related protein 1 (LRP-1). *PLoS One* 2013;**8**:e64145.

[30] Shin JH, Kim IY, Kim YN, Shin SM, Roh KJ, Lee SH, Sohn M, Cho SY, Lee SH, Ko CY, et al. Obesity resistance and enhanced insulin sensitivity in Ahnak-/- Mice fed a high fat diet are related to impaired adipogenesis and increased energy expenditure. *PLoS One* 2015;**10**:e0139720.

[31] Kim IY, Jung J, Jang M, Ahn YG, Shin JH, Choi JW, Sohn MR, Shin SM, Kang DG, Lee HS, et al. 1H NMR-based metabolomic study on resistance to diet-induced obesity in AHNAK knock-out mice. *Biochem Biophys Res Commun* 2010;**403**:428–34.

[32] Shin S, Seong JK, Bae YS. Ahnak stimulates BMP2-mediated adipocyte differentiation through Smad1 activation. *Obesity (Silver Spring)* 2016;**24**:398–407.

[33] Stopsack KH, Gerke TA, Andren O, Andersson SO, Giovannucci EL, Mucci LA, Rider JR. Cholesterol uptake and regulation in high-grade and lethal prostate cancers. *Carcinogenesis* 2017;**38**:806–11.

[34] Wang B, Rong X, Palladino END, Wang J, Fogelman AM, Martin MG, Alrefai WA, Ford DA, Tontonoz P. Phospholipid remodeling and cholesterol

availability regulate intestinal stemness and tumorigenesis. *Cell Stem Cell* 2018;**22**:206–20 e204.

[35] Ruscica M, Ricci C, Macchi C, Magni P, Cristofani R, Liu J, Corsini A, Ferri N. Suppressor of Cytokine Signaling-3 (SOCS-3) Induces Proprotein Convertase Subtilisin Kexin Type 9 (PCSK9) Expression in Hepatic HepG2 Cell Line. *J Biol Chem* 2016;**291**:3508–19.

[36] Macchi C, Ferri N, Sirtori CR, Corsini A, Banach M, Ruscica M. Proprotein Convertase Subtilisin Kexin Type 9: A View beyond the Canonical Cholesterol-Lowering Impact. *Am J Pathol* 2021;**191**:1385–97.

[37] Liu X, Bao X, Hu M, Chang H, Jiao M, Cheng J, Xie L, Huang Q, Li F. Inhibition of PCSK9 potentiates immune checkpoint therapy for cancer. *Nature* 2020;**588**:693–8.